Arch. Metall. Mater. **64** (2019), 4, 1653-1659

DOI: 10.24425/amm.2019.130140

K. SZMIGIELSKA*#, M. TRZASKA*

STRUCTURE AND PROPERTIES OF Zn/MoS_2 COMPOSITE COATINGS PRODUCED BY ELECTROCHEMICAL REDUCTION

The report presents research efforts on the synthesis of Zn/MoS_2 composite coatings by electrochemical reduction from a sulphate-borate bath containing MoS_2 powder as a dispersion phase at various concentrations. The structure of the Zn/MoS_2 composite coatings was characterised and the effect of MoS_2 particles embedded on their microhardness was evaluated. The coatings produced are characterized by a compact, homogeneous structure and a good connection to a steel substrate. The incorporation of MoS_2 particles into the zinc matrix has an influence on the structure and morphology of the Zn/MoS_2 composite coatings. It was found that the presence of MoS_2 particles increases surface roughness along with coating hardness. The incorporation of the MoS_2 particles into the zinc matrix slightly improves the corrosion resistance compared to Zn coatings, making the corrosion potential shift towards more electropositive values.

Keywords: electrodeposition, zinc coating, Zn/MoS_2 composites

1. Introduction

Zinc-based coatings have been widely applied in the corrosion protection of steel substrates since the 1960s [1]. The protection acts both as a physical barrier of the substrate from the corrosive environment and its self-sacrificial anodic protection coating. A number of applications of the Zn coatings ranges from the automobile industry and general mechanics to electronic components and construction pieces [2-3]. A wide range of these applications arises from low manufacturing costs of zinc protecting layers and their sufficient physical and chemical properties.

In the recent years a great research progress have been made to electrodeposit Zn coatings from various electroplating baths containing different dispersive phases which aim to improve the structure and properties of the deposit [4-6]. The latter include morphology, microhardness, wear resistance and corrosion resistance. A number of dispersed phases were studied which include both soft phases, such as polytetrafluoroethylene (PTFE), graphene and hard phases, such as Al_2O_3, TiO_2, SiC and, Si_3N_4 [7-17]. Recently, insoluble MoS_2 particles have been reported as a promising phase to enhance the corrosion resistance of the Zn/MoS_2 composite coatings [15].

MoS_2 was applied before in the electrodeposition of other metal matrices, including Ni and Cu and was shown to enhance the strength of a final coating for good wear resistance [18-20] and better self-lubrication properties [21]. These phenomena were explained by the modification of the final coating surface by engulfed soft MoS_2 particles during the conventional electroplating process. Y. He et al. [21] confirmed that the MoS_2 addition reduced the friction of the resultant coating. The lower friction coefficient of the final material was achieved when the higher amount of MoS_2 was incorporated. A new applications of Zn/MoS_2 composite films are explored and there are some promising reports of their potential use as an efficient catalyst for the production of biodiesel from Soybean Oil [22].

The aim of the present study is twofold: (1) probing the electrodeposition of Zn/MoS_2 composite coatings from sulphate-borate baths containing various concentrations of dispersed MoS_2 powder and (2) characterizing obtained coatings in terms of their morphology and texture, roughness, microhardness and the corrosion resistance.

2. Materials and methods

The research material concerned of zinc and composite Zn/MoS_2 coatings produced by electrochemical reduction in an acidic bath (pH 3.0) composed of zinc sulphate, aluminium sulphate, sodium sulphate, and boric acid. In order to deposit the Zn/MoS_2 composite coatings, MoS_2 particles, as a dispersed phase, were added to the bath in the concentration of 2.5, 5.0, 7.5 or 10.0 g/dm^3, respectively. High purity reagents from Sigma-Aldrich, Avantor Performance Materials Poland SA (formerly P.P.H. POCh Gliwice), Aldrich Chemical Co. Ltd and Chempur® were used for the preparation of the bath. The

* ŁUKASIEWICZ RESEARCH NETWORK – INSTITUTE OF PRECISION MECHANICS, UL. DUCHNICKA 3, 01-796 WARSAW, POLAND

Corresponding author: katarzyna.szmigielska@imp.edu.pl

zinc and Zn/MoS_2 composite coatings were deposited onto the surface of S235JR constructional carbon steel. The substrate was ground with a sandpaper of granulation of 400, 600 and 800, respectively, than degreased with calcium carbonate, rinsed in distilled water, activated with the aqueous (1:1) hydrochloric acid and rinsed.

The electrodeposition of zinc and Zn/MoS_2 coatings was carried out under constant current conditions at a current density of 3 A/dm^2 at the ambient temperature. Zinc anodes were used for the deposition process, with an anode-to-cathode surface ratio equal 2.5:1. The laboratory power supply (DF173005C NDN) was used as a current source. During the process, the mechanical mixing of the solution at 200 r.p.m. was applied (50D CAT). The deposition time was 50 minutes.

The morphology of the MoS_2 powder and the morphology and topography of Zn and Zn/MoS_2 coatings along with the structure of the produced coatings and their chemical composition were analyzed by means of Scanning Electron Microscope (SEM) coupled to the energy dispersive spectroscopy (EDS) analyzer (JSM-IT100 JEOL). For SEM imaging SE detector was used with the voltage of 15.0 kV. The thickness and coatings connection with a substrate were characterized on cross-sections perpendicular to the surface of Zn and Zn/MoS_2 coatings using a light microscope (LM) with the digital image processing (VHX 5000 KEYENCE).

The X-ray fluorescence spectrophotometer was used to analyze the chemical composition of the coatings (i.e., determination of the content of individual elements) and to measure their thickness (X-RAY XDV-SDD FISCHER X-RAY FESCHERSCOPE®). The roughness parameters Ra (arithmetical mean deviation of the assessed profile) and Rz (average distance between the five highest peaks and lowest valleys over the entire sampling length) (Surftest SJ-210P MITUTOYO) and Knoop microhardness at a load of 10 G (HK 0.01) (Tukon™ 1202 WILSON-HARDNESS) of zinc and composite coatings produced were also determined.

Electrochemical tests of the corrosion properties were carried out in 0.5 M NaCl solution at 22 ± 2°C. Tests were performed in a three-electrode system in which the test electrode was a Zn or Zn/MoS_2 coating, the counter electrode was a platinum mesh, and a Standard Calomel electrode (SCE) was used as a reference electrode. The research was carried out using a low-amplitude polarization with an SP-200 set (BIO-LOGIC). A potential ranged from –250 mV to +250 mV versus Open Circuit Potential (OCP). The scanning speed was 0.001 V/s. To determine the corrosion current density (j_{corr}) and corrosive potential (E_{corr}), the extrapolation method tangent to the polarization curves $E = f(j)$ from the cathodic and anodic regions was used.

3. Results and discussion

To the best of our knowledge, so far the electrodeposition of Zn/MoS_2 composite coatings was only conducted from chloride baths [15]. To produce composite coatings, the MoS_2 powder was applied as a dispersed phase. The image of the MoS_2 powder (SEM) is shown in Fig. 1. The MoS_2 particles have different shape with dimensions below 3 μm.

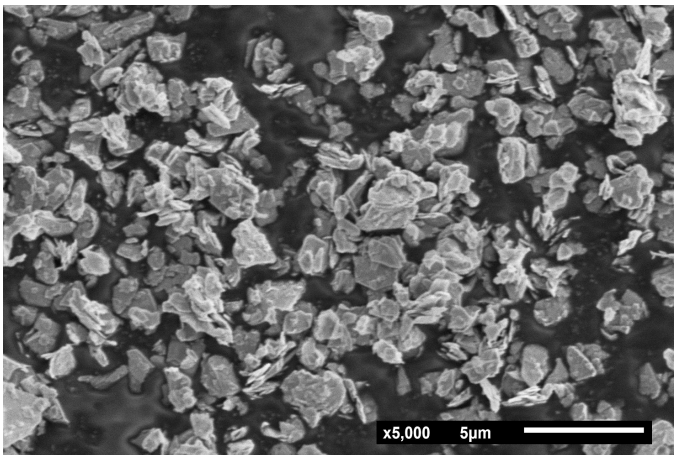

Fig. 1. Image of MoS_2 powder particles (SEM)

Composite coatings with a zinc matrix were prepared from baths containing the MoS_2 powder at the concentration of 2.5, 5.0, 7.5 and 10.0 g/dm^3, respectively. For the comparison purposes, the pure zinc coating was also deposited.

The Zn deposit was light grey. However, while Zn/MoS_2 composite coatings were characterized by a darker gray colour, which deepen with an increasing content of the embedded MoS_2 particles.

The average thickness of the zinc coating produced was about 33 μm. However, the Zn/MoS_2 composite coatings were characterized by an average thickness of *ca*. 30 μm. There was no significant effect of MoS_2 particle concentration on the thickness of the composite coatings. The thickness values determined with an XRF method and on the cross-sections correlate with each other.

The images of the surface morphology and surface topography of zinc and composite coatings recorded with the SEM are shown in Figures 2 and 3.

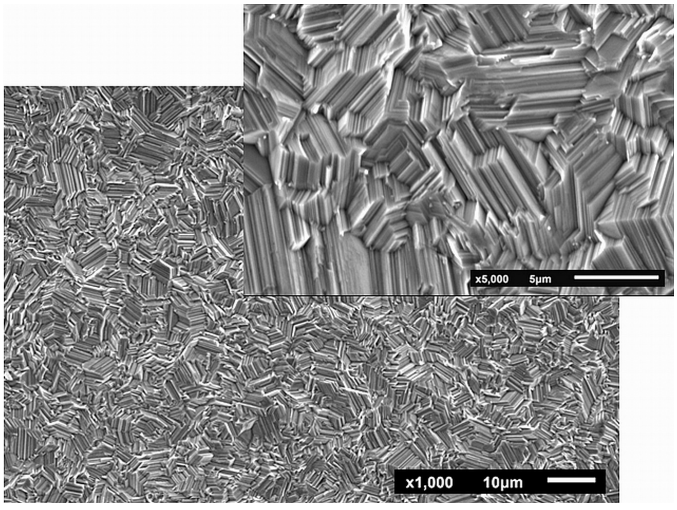

Fig. 2. Surface morphology of zinc coating (SEM)

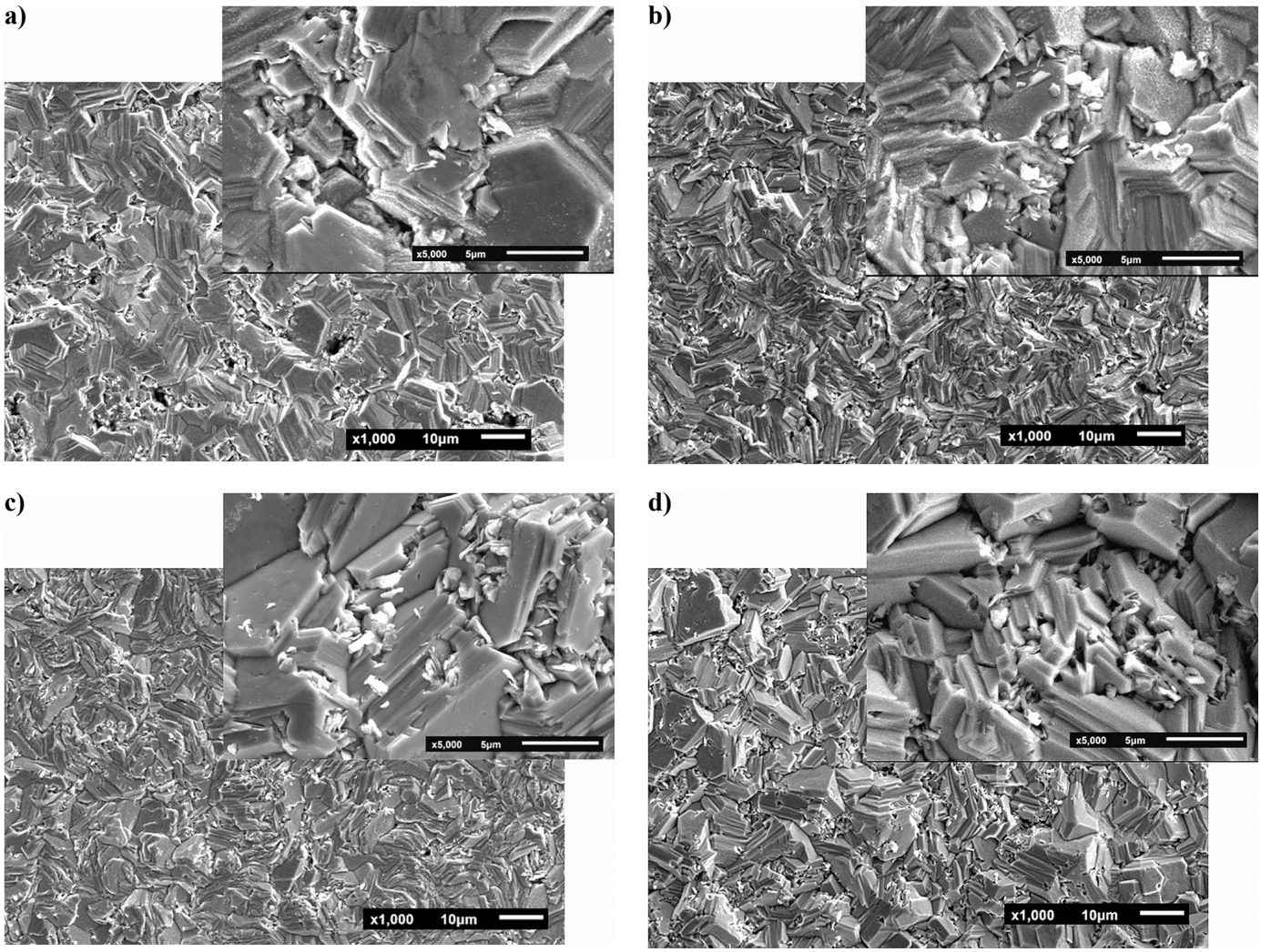

Fig. 3. Surface morphology of Zn/MoS_2 composite coating obtained from the bath containing (a) 2.5; (b) 5.0; (c) 7.5, and (d) 10.0 g/dm^3 (SEM)

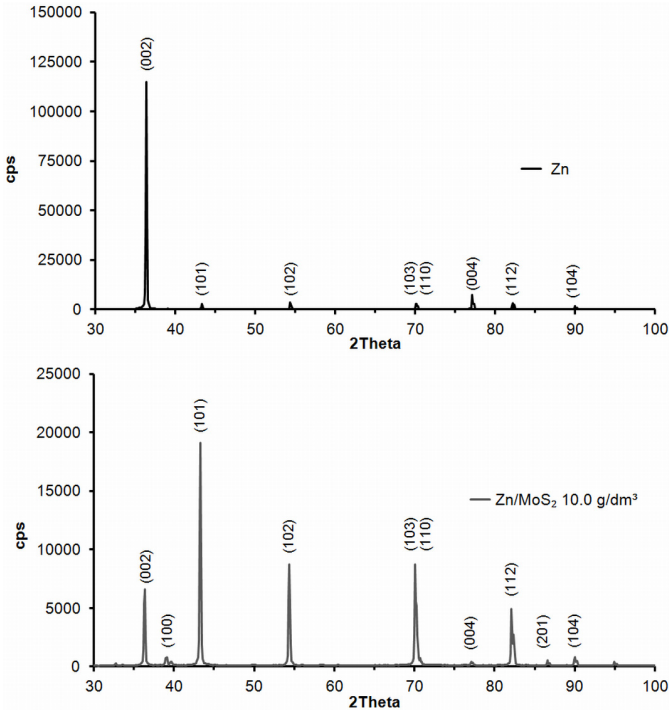

Fig. 4. The XRD pattern of Zn and Zn/MoS_2 composite coatings

The Zn and Zn/MoS_2 composite coatings exhibit a crystalline structure. The XRD pattern of produced coatings are shown in Figure 4.

The incorporation of MoS_2 into zinc matrix has an effect on the orientation of zinc crystallites from the plane (002) for pure zinc coating to the plane (101) for composite coating. This was also observed by V. Kanagalasara et al. [15]. The incorporation of the MoS_2 disperse phase into the zinc coating increases the surface development.

The results of the Mo content measurement (w/w %) in the Zn/MoS_2 composite coating material obtained with the XRF spectra analysis are summarized in Table 1. The content of a dispersion phase in the coating was dependent on the MoS_2 concentration in the bath and increases with the concentration of a dispersed phase in the bath. The lowest MoS_2 content in the coating was observed for the Zn/MoS_2 coating produced in a bath with the MoS_2 phase concentration of 2.5 g/dm^3 and constituted about 0.6 wt%. However, the highest MoS_2 content in the Zn/MoS_2 coating was noted when deposition was carried out from a bath containing the MoS_2 phase at the concentration of 10.0 g/dm^3. The resultant Zn/MoS_2 coating contained *ca.* 1.0 wt% of a dispersion phase.

TABLE 1

Molybdenum [wt%] content in the Zn/MoS_2 composite coatings (XRF)

Coating	Mo content in the coating [wt%]	Standard deviation [wt%]
Zn/MoS_2 (2.5 g/dm^3)	0.6	0.3
Zn/MoS_2 (5.0 g/dm^3)	0.8	0.2
Zn/MoS_2 (7.5 g/dm^3)	0.9	0.2
Zn/MoS_2 (10.0 g/dm^3)	1.0	0.1

The images of the decomposition of zinc, molybdenum and sulphur in a surface layer of Zn/MoS_2 composite coatings produced from a bath containing different amounts of MoS_2 are summarized in Fig. 5. The agglomerates of the incompletely embedded MoS_2 dispersion phase are clearly visible onto the surface of the composite coatings. This phenomenon was more pronounced onto the surface of the Zn/MoS_2 composite coating produced from a bath with the MoS_2 phase concentration of 10.0 g/dm^3.

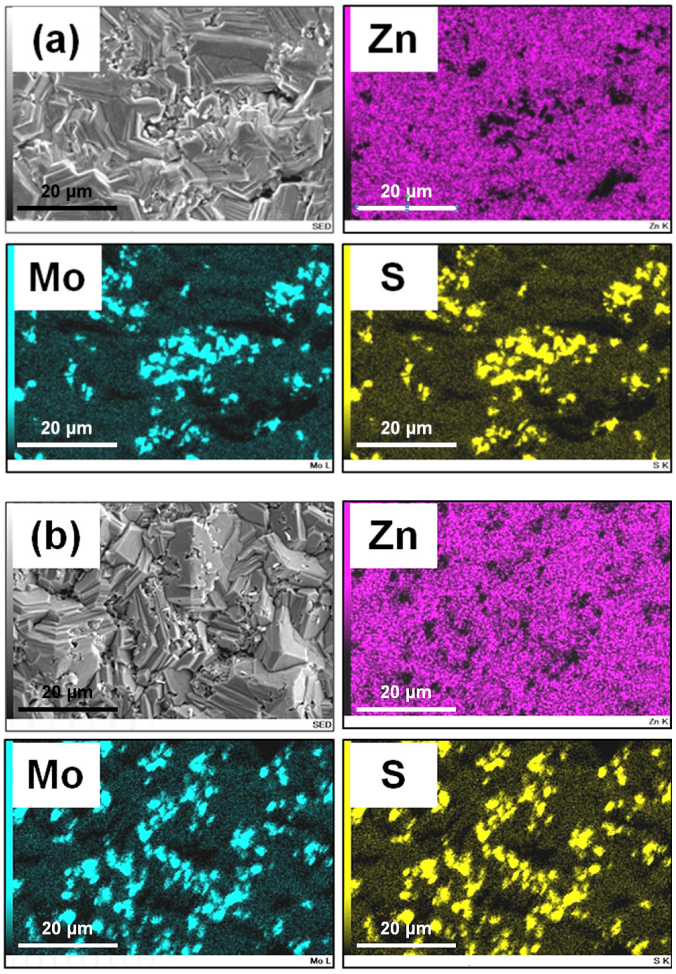

Fig. 5. The SEM image and distribution of zinc, molybdenum and sulphur on the surface of the Zn/MoS_2 composite coating obtained from the bath containing (a) 2.5, and (b) 10.0 g/dm^3 MoS_2 dispersed phase

The images of cross-sections perpendicular to the surface of the zinc and composite Zn/MoS_2 coatings obtained from a bath containing 2.5, 5.0, 7.5 and 10.0 g/dm^3, respectively, are shown in Fig. 6 and 7. Both the zinc coating and the Zn/MoS_2 composite coatings were characterized by the compact structure, even thickness on a covered surface and good connection to a steel substrate.

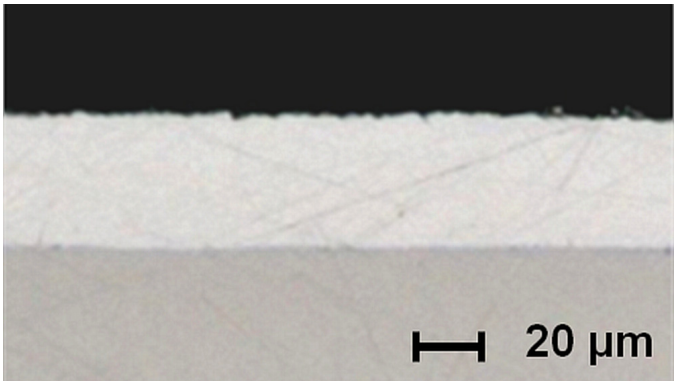

Fig. 6. The cross-sections of zinc coatings (LM)

An exemplary molybdenum and sulphur distribution on cross-sections perpendicular to the surface of the Zn/MoS_2 composite coating prepared from a bath containing 2.5 g/dm^3 of the MoS_2 dispersed phase particles is shown in Fig. 8.

The EDS analysis of the molybdenum and sulphur distribution on the cross-section of the Zn/MoS_2 composite coating confirmed the incorporation of a dispersed phase into the volume of the matrix material. The cross-section of the composite coating displays the agglomerates of the MoS_2 powder.

The results of the roughness measurements of the zinc coating and Zn/MoS_2 composite coatings are shown in Table 2. The Zn/MoS_2 composite coatings were characterized by an enhanced surface development compared to the zinc ones. The highest roughness was observed for the composite coatings produced from a bath containing the MoS_2 particles at the concentration of 7.5 and 10.0 g/dm^3, respectively.

TABLE 2

Roughness parameters (*Ra* and *Rz*) of zinc and Zn/MoS_2 composite coatings. Length of the measuring section λ_c = 0,8 mm

Coating	*Ra* [µm]	Standard deviation [µm]	*Rz* [µm]	Standard deviation [µm]
Zn	0.5	0.1	3.6	0.7
Zn/MoS_2 (2.5 g/dm^3)	1.0	0.2	6.9	1.6
Zn/MoS_2 (5.0 g/dm^3)	1.1	0.2	7.7	0.8
Zn/MoS_2 (7.5 g/dm^3)	1.2	0.1	8.3	1.0
Zn/MoS_2 (10.0 g/dm^3)	1.2	0.2	8.5	1.2

The Knoop microhardness determined on the surface of zinc and Zn/MoS_2 coatings are shown in Table 3. The microhardness measurements showed that in the studied range of dispersed phase concentrations the incorporation of the MoS_2 particles into the zinc matrix led to the slightly strengthened coatings.

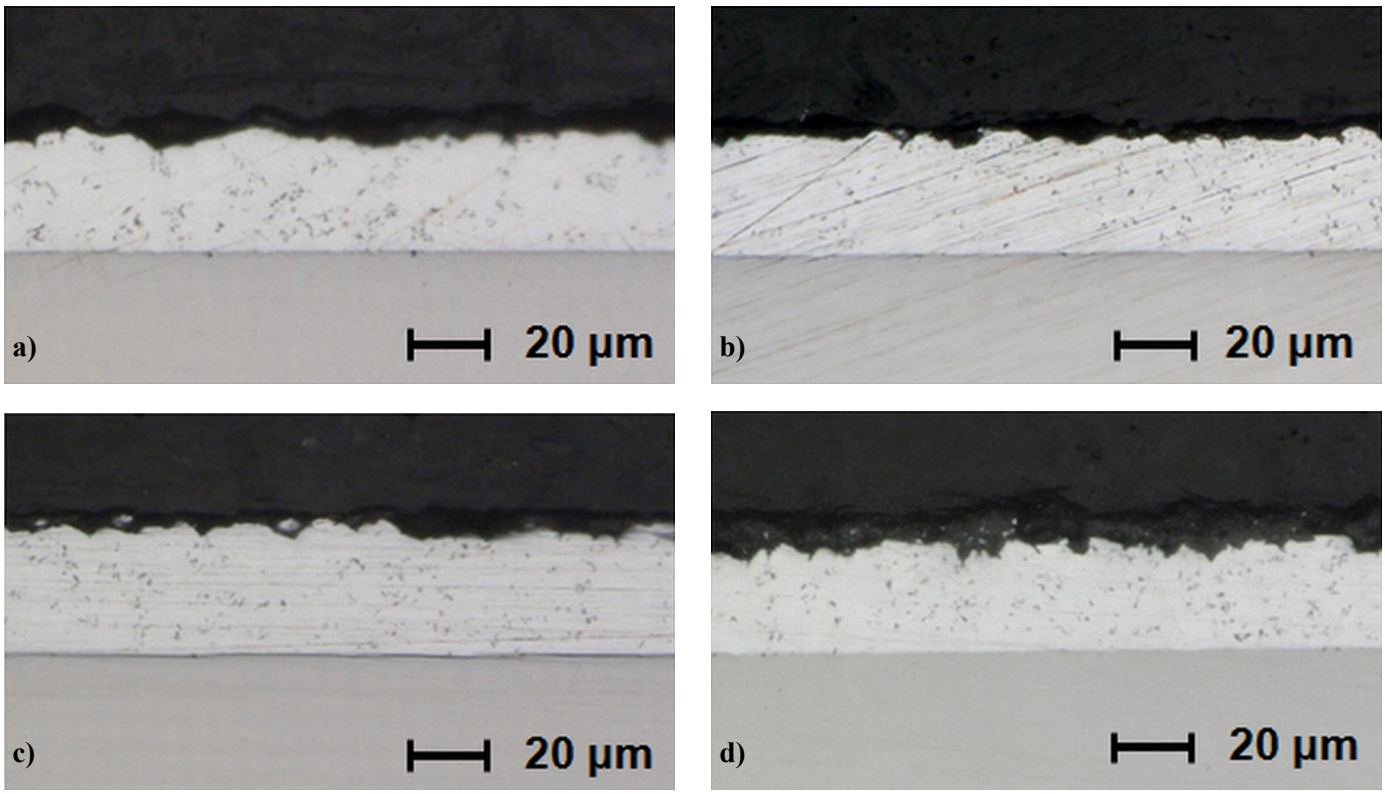

Fig. 7. The cross-sections of Zn/MoS_2 composite coatings obtained from the bath containing: (a) 2.5; (b) 5.0; (c) 7.5 and (d) 10.0 g/dm^3 MoS_2 (LM)

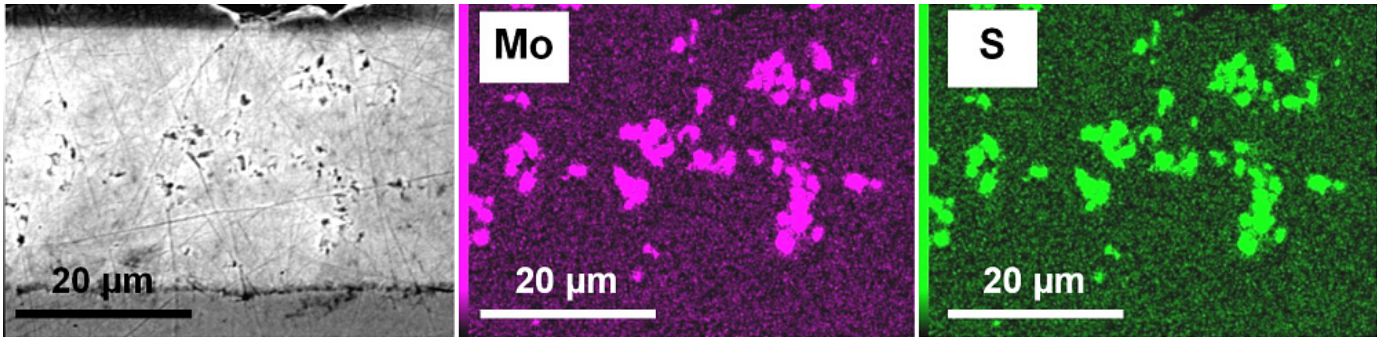

Fig. 8. SEM image and distribution of molybdenum and sulphur on the cross-section of the Zn/MoS_2 composite coating, produced in a bath containing 2.5 g/dm^3 of MoS_2

TABLE 3

Knoop microhardness of Zn and Zn/MoS_2 composite coatings

Coating	HK 0.01	Standard deviation
Zn	41	6
Zn/MoS_2 (2.5 g/dm^3)	40	4
Zn/MoS_2 (5.0 g/dm^3)	43	3
Zn/MoS_2 (7.5 g/dm^3)	45	4
Zn/MoS_2 (10.0 g/dm^3)	55	4

The highest increase of the microhardness by *ca.* 30% compared to the zinc coating was observed for the Zn/MoS_2 composite coating, produced from a bath containing a dispersed phase at the concentration of 10.0 g/dm^3.

The corrosion properties of the coatings produced were examined by an electrochemical dynamic potential method. The potentiodynamic polarization curves recorded for the Zn coating and Zn/MoS_2 composite coatings are shown in Fig. 9. Table 4 summarizes both the corrosion potential and corrosion current determined using an extrapolation method tangent to the Tafel curves.

TABLE 4

Corrosion potential and corrosion current of Zn and Zn/MoS_2 composite coatings

Coating	E_{corr} [mV]	I_{corr} [μA/cm^2]
Zn	–1039.4	8.3
Zn/MoS_2 (2.5 g/dm^3)	–1009.5	22.1
Zn/MoS_2 (5.0 g/dm^3)	–997.8	28.2
Zn/MoS_2 (7.5 g/dm^3)	–1038.5	20.6
Zn/MoS_2 (10.0 g/dm^3)	–1019.4	25.4

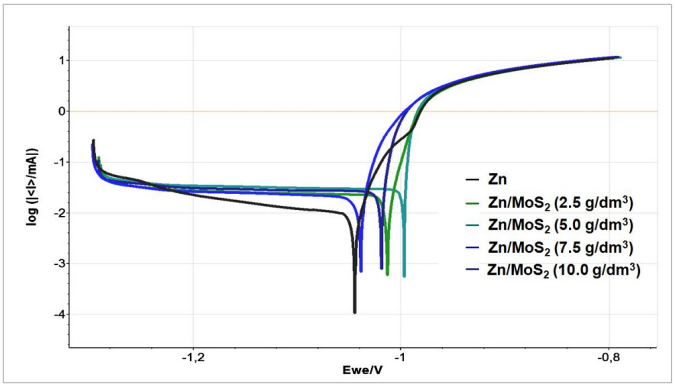

Fig. 9. Polarization curves of Zn coating and Zn/MoS_2 composite coatings

The polarization curves obtained for the composite coatings exhibit a similar trend, which however, seem to slightly differ from the polarization curve obtained for the pure zinc coating. A shift of the corrosion potentials of the Zn/MoS_2 composite coatings towards less negative potentials was observed in comparison to the corrosion potential for the zinc coating. A highest shift towards the more electropositive potentials was found for the composite coating obtained from a bath containing 5.0 g/dm^3 of the MoS_2 powder. The produced composite coatings are characterized by a greater degree of the surface development compared to the zinc coating, which by far affects the course of the corrosion processes. Fig. 10 and Fig. 11 show the surface images of the produced coatings upon the corrosion tests.

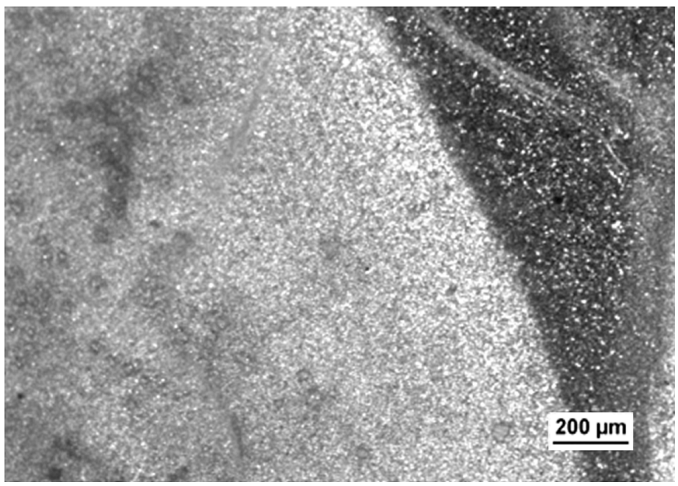

Fig. 10. Surface morphology of Zn coatings after corrosion tests (LM)

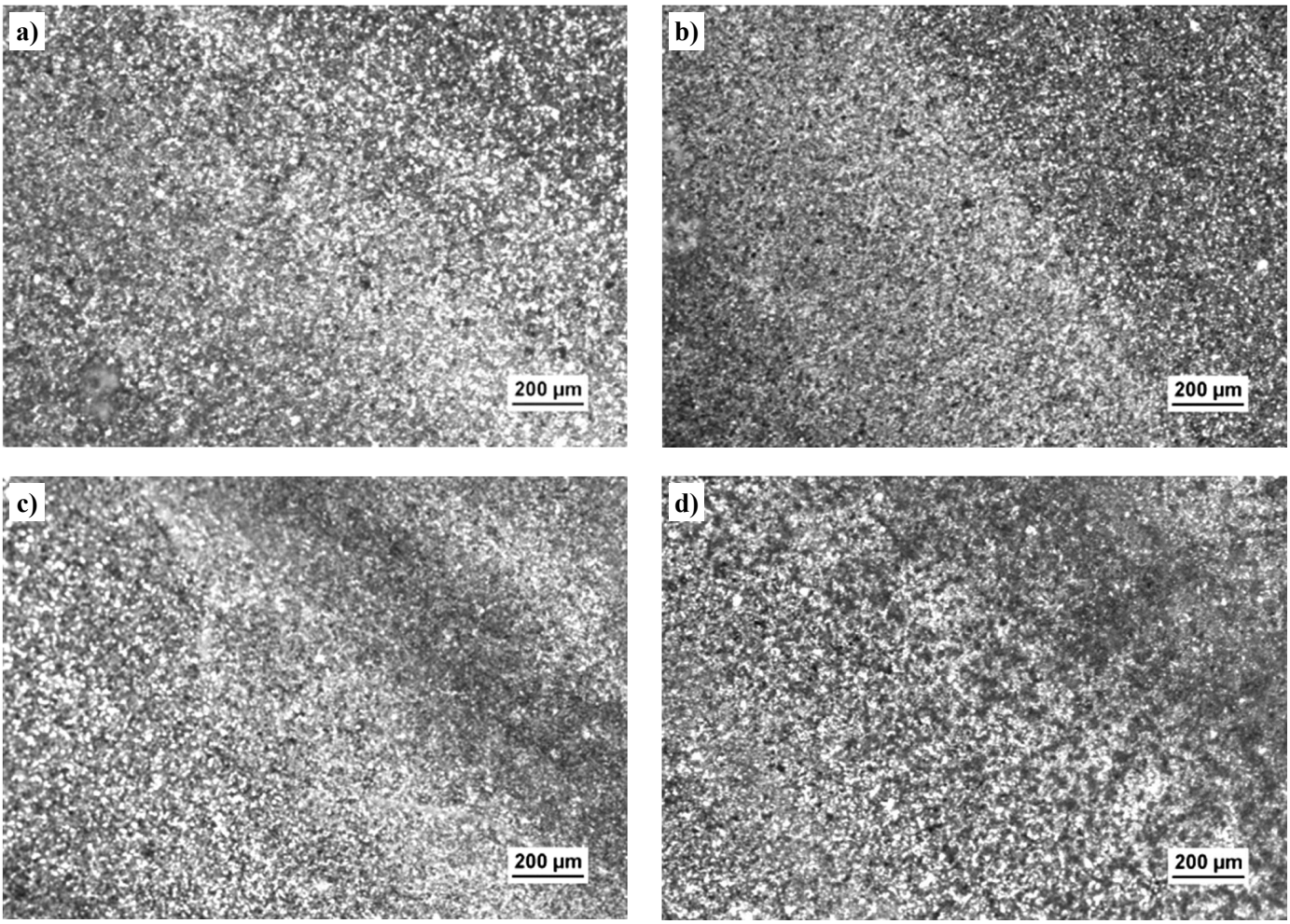

Fig. 11. Surface morphology after corrosion tests of Zn/MoS_2 composite coatings obtained from the bath with MoS_2 concentration: (a) 2.5, (b) 5.0, (c) 7.5, and (d) 10.0 g/dm^3 (LM)

The surface morphology of the Zn and Zn/MoS_2 coatings after the corrosion tests indicates uniform corrosion. In addition, no pitting formation was observed.

4. Summary

The Zn/MoS_2 composite coatings were deposited from an acidic sulphate-borate bath containing the MoS_2 powder as a dispersed phase at the concentrations of 2.5, 5.0, 7.5 and 10.0 g/dm^3, respectively. Within this concentration range, an increase of the MoS_2 concentration in the bath leads to a slight increase of the MoS_2 content in the coating. The coatings produced contained from *ca.* 0.6 wt%. up to 1.0 wt% of molybdenum sulphide. The Zn and Zn/MoS_2 coatings were characterized by a compact structure, the uniform thickness on a covered surface. The average thickness was about 30-33 μm. The addition of the MoS_2 dispersed phase into a bath resulted in a reduction of the efficiency of the deposition process by *ca.* 9%.

In the applied range of dispersed phase concentrations, the incorporation of a soft MoS_2 phase into zinc matrix resulted in an increase of the roughness parameters and a slightly increase of the microhardness of these coatings compared to the pure zinc coating.

The conducted corrosion tests showed that the incorporation of MoS_2 particles into zinc coatings slightly elevated the corrosion resistance compared to the Zn coating. However, further research is needed to evaluate these problems in more detail.

REFERENCES

[1] F.C. Walsh, C.P. de León, Trans. Inst. Meter. Finish. **92**, 83-98 (2014), DOI: 10.1179/0020296713Z.000000000161.

[2] Fashu, Simbarashe; Khan, Rajwali, Anti-Corros. Methods Mater. **66** (1), 45-60 (2019), DOI:10.1108/ACMM-06-2018-1957.

[3] Zhiqiang Gao, Dawei Zhang, Zhiyong Liu, Xiaogang Li, Shemming Jiang, Qifu Zhang, J. Coat. Technol. Res. **16** (1), 1-13 (2018), DOI: 10.1007/s11998-018-0076-1.

[4] X. Xia, I. Zhitomirsky, J.R. McDermid, J. Mat. Proces. Technol. **209**, 2632-2640 (2009), DOI: 10.1016/j.jmatprotec.2008.06.031.

[5] M. Ilieva, S. Ivanov, V. Tsakova, J. App. Electrochem. **38**, 63-69 (2008), DOI: 10.1007/s10800-007-9399-9.

[6] H. Zheng, A.N. Maozhong, L.U. Junfeng, Rare Metals **25**, 174-178 (2006), DOI: 10.1016/S1001-0521(08)60076-5.

[7] G. Roventi, T. Bellezze, R. Fratesi, J. Appl. Electrochem. **43**, 839-846 (2013), DOI: 10.1007/s10800-013-0571-0.

[8] P. Drasnar, J. Kudlacek, V. Kreibich, V. Kracmar, M. Vales, MM Science Journal, 248/249 (2011), DOI : 10.17973/MMSJ.2011_07_201106.

[9] M. Pazderova, M. Bradac, M. Vales; MM Science Journal, 208/209 (2010), DOI : 10.17973/MMSJ.2010_11_201016.

[10] P.C. Tulio, I.A. Carlos, J. Appl. Electrochem. **39**, 1305-1311 (2009), DOI: 10.1007/s10800-009-9803-8.

[11] J. Fustes, A. Gomes, M. I. da Silva Pereira, J. Solid State Electrochem. **12**, 1435-1443 (2008), DOI: 10.1007/s10008-007-0485-z.

[12] A. Sachian, M. Blidariu, E. Roman, C. Raducanu, Trans. Inst. Metal Finish. **75** (6), 213-215 (1997), DOI: 10.1080/00202967.1997.11871176.

[13] P. Miceli, V. John, Production and properties of electrolytically deposited novel alloy coatings on steel; Report, (EUR 18384), European Commission, Luxembourg (1998).

[14] J. Kubicki, B. Szczygieł, Protective coatings (Powłoki Ochronne), **1-2** (59-60), 27-32 (1983).

[15] Vathsala Kanagalasara, Thimmappa Venkatarangaiah Venkatesha, J. Solid State Electrochem. **16**, 993-1001 (2012), DOI: 10.1007/s10008-011-1475-8.

[16] K. Szmigielska, W. Bartoszek, M. Trzaska, Surface Engineering (Inżynieria Powierzchni), **25** (4), 42-47 (2018), DOI: 10.5604/01.3001.0012.9801.

[17] M.K. Punith Kumar, Mahander Pratap Singh, Candan Srivastava, RSC Adv. **5**, 25603-25608 (2015), DOI10.1039/c5ra02898a.

[18] V.C. Fox, N. Renevier, D.G. Teer, J. Hampshire, V. Rigato, Surf. Coat. Technol. **116-119**, 492-497 (1999) DOI: 10.1016/S0257-8972(03)00247-0.

[19] N.M. Renevier, H. Oosterling, U. Konig, H. Dautzenberg, B.J. Kim, L. Geppert, F.G.M. Koopmans, J. Leopold, Surf. Coat. Technol. **172**, 13-23 (2003), DOI: 10.1016/j.tsf.2009.03.210.

[20] R.L. Jeffrey, I.K. Hyun, M.A. Paul, J.D. Daniel, T.D. Michael, Thin Solid Films, **517**, 5516-5522 (2009), DOI: 10.1016/j.tsf.2009.03.210.

[21] Y. He, S.C. Wang, F.C. Walsh, Y.-L. Chiu, P.A.S. Reed, Surf. Coat. Technol. **307**, 926-934 (2016), DOI: 10.1016/j.surfcoat.2016.09.078.

[22] Z. Huang, H. Sun, H. Gao, X. Pei, S. Wei, J. Electrochem. Sci. **12**, 7702-7711 (2017), DOI: 10.20964/2017.08.03.